

# Improving Burst Alignment in TOPS Interferometry With Bivariate Enhanced Spectral Diversity

Kang Wang<sup>✉</sup>, Xiaohua Xu, and Yuri Fialko

**Abstract**—Terrain observation by progressive scans (TOPS)-mode synthetic aperture radar interferometry requires high accuracy of burst alignments. Geometrical burst alignment relying on precise orbits and digital topography is not always sufficient for Sentinel-1A TOPS-mode interferometry. Enhanced spectral diversity (ESD) method was proposed to estimate a constant azimuth shift between radar images that minimizes phase discontinuities across the bursts. In some cases, however, the ESD refinement fails to align the bursts in Sentinel-1 interferograms, possibly because of ionospheric propagation effects. Here, we show that in such cases, a bivariate shift (that depends on both azimuth and range) can efficiently remove phase discontinuities across the bursts. The bivariate shift can be derived from the double-differenced radar phase in the burst overlap regions.

**Index Terms**—Burst alignment, enhanced spectral diversity (ESD), ionospheric delays, Sentinel-1, terrain observation by progressive scans (TOPS) synthetic aperture radar (SAR).

## I. INTRODUCTION

SEVERAL current synthetic aperture radar (SAR) missions, including Sentinel-1 and TerraSAR-X, employ terrain observation by progressive scans (TOPS)-mode [3]. In the TOPS-mode SAR system, the antenna is rotated from backward- to forward-looking direction during the burst acquisition (opposite to the antenna rotation in case of the SPOT-mode SAR system). While this approach improves the image quality both in terms of amplitude (decreased “scalloping” effect) and phase (reduced azimuth ambiguity), the fast steering of antenna along the azimuth direction causes large variations of the Doppler centroid within a burst [3]. It is well known that in the presence of a squint, linear phase ramps are introduced in the focused response both in azimuth and range, although ramps in the range direction are mostly negligible. To form interferograms of coherent phase, the reference and repeat images have to be aligned accurately. However, because the orbital velocities or burst timing of the reference and repeat acquisitions may be different, a small misalignment of bursts in the azimuth direction could be expected. As the difference in the Doppler centroids at the upper and lower edges of

Manuscript received September 22, 2017; accepted October 23, 2017. Date of publication November 17, 2017; date of current version December 4, 2017. This work was supported by the National Aeronautics and Space Administration under Grant NNX14AQ15G. (*Corresponding author:* Kang Wang.)

The authors are with the Institute of Geophysical and Planetary Physics, Scripps Institution of Oceanography, University of California at San Diego, La Jolla, CA 92037 USA (e-mail: kjellywang@gmail.com).

This paper has supplementary downloadable material available at <http://ieeexplore.ieee.org>, provided by the author.

Color versions of one or more of the figures in this letter are available online at <http://ieeexplore.ieee.org>.

Digital Object Identifier 10.1109/LGRS.2017.2767575

each burst is usually much larger than the pulse repetition frequency (PRF), a small azimuthal misalignment could result in a significant phase jump in the interferogram at the burst boundaries. The relationship between the burst misalignment  $\Delta a$  and the resulting phase jump  $\phi$  at the burst boundaries is

$$\Delta a = \text{PRF} \frac{\phi}{2\pi \Delta f} \quad (1)$$

where  $\Delta f$  denotes the Doppler centroid variation caused by steering of the antenna from backward-looking to forward-looking within one burst [9], [13]. For example, for the C-band Sentinel-1 mission, the Doppler centroid variation within one burst is  $\sim 4500$  Hz, and the effective PRF is 486 Hz. Therefore, to keep phase jumps to be smaller than 1/10 of a phase cycle (corresponding to 2.8 mm along the radar line of sight) at the burst boundaries, the burst alignment between reference and repeat acquisitions has to be at the accuracy of  $\sim 0.01$  pixel size in the azimuth direction. The traditional cross correlation method used in the stripmap mode SAR interferometry is not sufficient for this purpose. With the information on SAR system’s internal geometry, satellite’s orbits, and external digital elevation model (DEM), one can precisely map the footprint of each image acquisition on the ground. Differencing the ground footprints provides an offset map needed for the image alignment. This method is often referred to as “geometrical alignment.” The accuracy of the geometrical alignment largely depends on the accuracy of satellite orbits. For the Sentinel-1 mission, the accuracy of the postprocessed orbit is  $\sim 5$ -cm along-track and  $\sim 2$ –3 cm radially and cross-track [5], i.e., on the order of 1% of the pixel size. While the geometrical alignment should in theory be sufficient for Sentinel-1 interferometry, in practice phase discontinuities between the bursts often persist.

The burst alignment can be improved by taking advantage of the fact that small overlapping regions between consecutive bursts are imaged twice from two slightly different view directions (forward-looking and backward-looking). Similar to the along-track interferogram or multiaperture interferogram in stripmap interferometry [1], [2], [11], a double-difference interferogram can be generated for pixels within the burst overlap regions. The double-differenced phase is proportional to the azimuth shift of pixels between image acquisitions. Provided that the ground motion along the satellite track is negligible between image acquisitions, the double-differenced phase of pixels in the burst overlap areas can be used to correct burst misalignment that might result from a clock drift, imprecise knowledge of satellite orbits or other unmodeled sources causing the along-track pixel shift. This method is

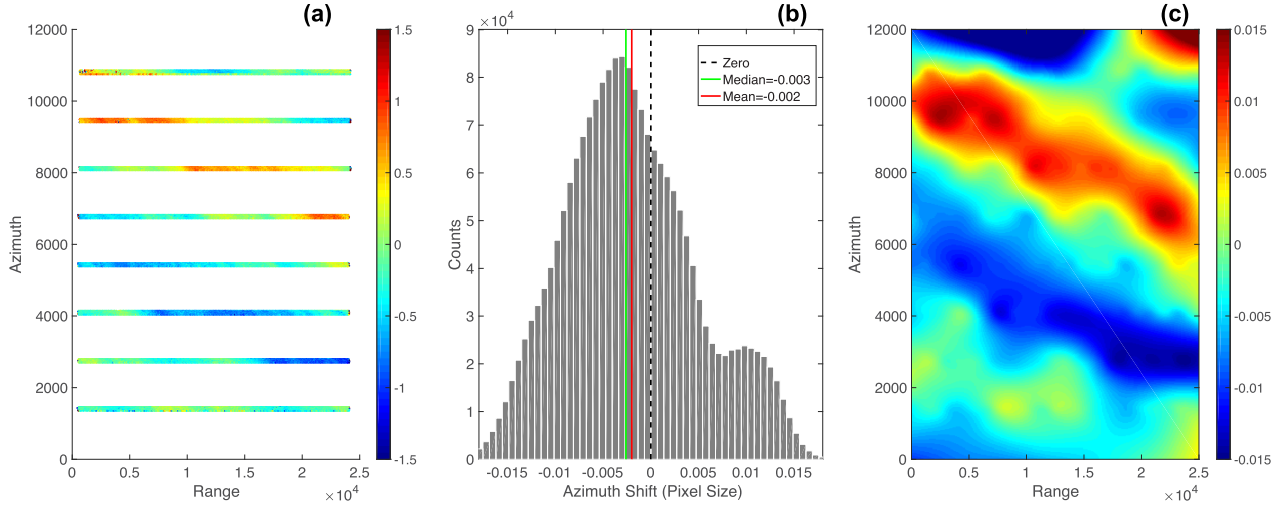


Fig. 1. (a) Double-differenced phase in the burst overlaps. (b) Histogram of azimuth shift for burst overlaps. (c) Interpolated azimuth shift map derived from the double-differenced phase from the burst overlap regions.

known as enhanced spectral diversity (ESD) [13] and is used in a number of data processing packages. SAR processors that use the ESD method to correct for the geometrical alignment use either median or mean values of the double-differenced phase within the burst overlap regions to estimate a constant shift in the azimuth direction. A few recent studies have attempted to use azimuth-dependent shift to correct for the geometrical misalignment [15], [17]. Here, we present examples of Sentinel-1A data that exhibit strong variations in the double-differenced phase in both range and azimuth directions. In such cases, corrections of burst alignments assuming a constant azimuth shift cannot completely remove artificial phase jumps at burst boundaries. We show that bivariate (azimuth- and range-dependent) azimuth shifts are necessary to produce accurate burst alignment in the TOPS-mode SAR interferometry.

## II. DATA PROCESSING

The data used in this letter are interferometric wide-swath TOPS-mode single look complexes of Sentinel-1A mission, downloaded from Alaska Satellite Facility. We processed the data with the latest (v5.2) version of GMT5SAR [18]. We first geometrically aligned the reference (master) and repeat (slave) images using the postprocessed precise orbit ephemerides and SRTM V3 3 arcsec DEM data. The double-differenced interferogram within the burst overlap regions was then calculated as follows:

$$\phi = \arg [(c_{11} \times c_{12}^*) \times (c_{21} \times c_{22}^*)^*] \quad (2)$$

where the first and second subscripts of each variable represent the view geometry and acquisition, respectively, and \* symbol represents the conjugate of a complex number. For instance,  $c_{22}^*$  denotes the conjugate of the complex numbers corresponding to forward-looking view in the second acquisition. We then calculated the azimuth shift of the burst overlap pixels using (1). Since the width of a burst overlap between two consecutive bursts is only about 1/10 of the width of a burst itself, interpolation is needed to fill gaps

between the bursts. To increase the signal-to-noise ratio, we applied a  $40 \times 10$  block median filter to the original double-differenced phase in the burst overlap regions before interpolation. We used a Laplacian operator to smooth the interpolation results. The degree of smoothing affects the final refinement of burst alignments. A weaker smoothing results in a better alignment. A stronger smoothing is more efficient at suppressing noise in the double-differenced phase that may give rise to spurious azimuth offsets. We tested a range of the smoothing parameters and chose an optimal value, such that the interpolated azimuth shift map is sufficiently smooth on the scales of 20 km or below, while the phase jumps across burst boundaries did not exceed 0.05 rad on average. The azimuth shift table after interpolation was then added to the shift table from geometrical alignment to refine the burst alignment.

## III. EXAMPLES

Here, we present an example to illustrate how the burst alignment can be improved with the bivariate (range-and-azimuth-dependent) ESD (BESD) method. For Sentinel-1 mission, each scene contains three subswaths and each subswath typically has nine bursts. For the sake of brevity and simplicity, in the following example, we only show a subswath with the largest phase discontinuities across burst boundaries after geometrical alignment. The SAR images used in this example cover an area in South America near the border of Chile, Bolivia, and Argentina. The area is characterized by high correlation of the radar phase due to an arid sparsely vegetated environment [6].

Fig. 1 shows the double-differenced phase for the burst overlaps pixels and its statistics (mean and median values). An obvious feature of the double-differenced interferogram in this example is a strong variation of the azimuth shift in both range and azimuth directions. The azimuth shift varies continuously from -0.015 to 0.015 across the swath, with the median and mean values of -0.0026 and 0.0019, respectively (see Fig. 1). Correspondingly, an interferogram with the geometrical burst alignment shows phase discontinuities across

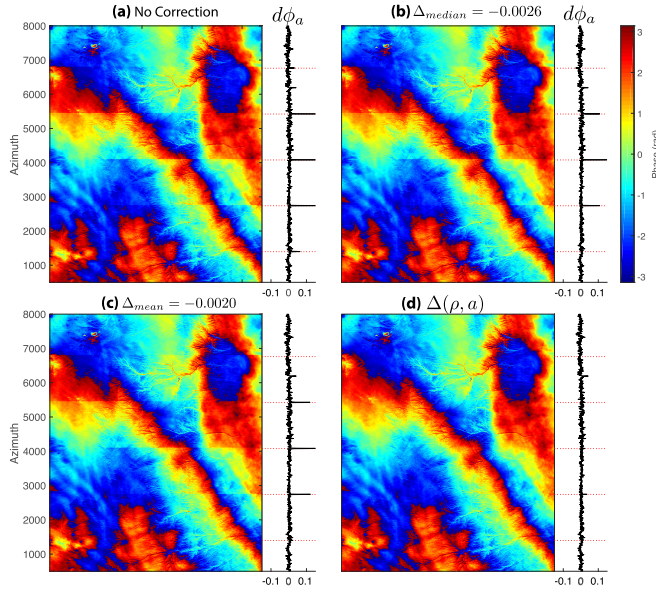


Fig. 2. (a) Geometrical alignment only. (b) Correction with median value of the azimuth shift derived using the ESD method. (c) Correction with mean value of the azimuth shift derived using the ESD method. (d) Correction with range-and-azimuth variable azimuth shift derived using the BESD method. The black profile to the right of each interferogram represents the average phase gradient along the azimuth direction. Phase discontinuities are manifested by spikes in the phase gradient. Red dotted lines: locations of burst boundaries.

most of the burst boundaries [see Fig. 2(a)]. To quantify phase jumps at burst boundaries, we computed an average phase gradient in the azimuth direction  $d\phi$  as

$$d\phi_j = \frac{1}{N} \sum_{i=1}^N [\phi(i, j+1) - \phi(i, j)] \quad (3)$$

where  $\phi$  denotes the unwrapped radar phase, indexes  $i$  and  $j$  denote pixel coordinates in range and azimuth, respectively, and  $N$  is the number of pixels in the range direction. The interferogram with no correction [see Fig. 2(a)] has an average phase jump of  $>0.1$  rad across most of the bursts (note that this value is the average phase jump along the range direction, and the local phase discontinuities across certain burst boundaries could be much higher than this value). The ESD corrections with the median and mean values of the azimuth shift from the double-difference interferogram do not appreciably reduce phase jumps between the bursts. On the other hand, the correction using a bivariate shift [network-based enhanced spectral diversity (NESD)] shown in Fig. 1(c) efficiently removes the phase discontinuities for the entire interferogram.

#### IV. DISCUSSION

Strong variations of the azimuth shift along both the range and azimuth directions suggest that such variations are unlikely due to clock errors or imprecise knowledge of satellite orbits. This is because clock and orbital errors might introduce variations in the azimuth shift that are chiefly azimuth-dependent. In addition, if the burst misalignment was due to the clock drift or orbital errors, the double-difference interferograms or equivalent azimuth shift maps

of all three subswaths would be expected to have nearly identical patterns of the azimuth dependence, as all subswaths are acquired from the same trajectory and at nearly the same time. To examine the pattern of the azimuth shift across different subswaths, we formed double-difference interferograms separately for each subswath of the SAR scenes used in the above-mentioned example. The combined double-differenced phase and inferred azimuth shift for all three subswaths are shown in Fig. 3. Both the original double-differenced phase in the burst overlap regions (see Fig. 3) and the interpolated azimuth shift [see Fig. 3(b)] show remarkable consistency and continuity across the subswath boundaries. The azimuth shift variations in the third subswath are on average much stronger than those in the first subswath, and are dominated by “ridges” and “troughs” that are oblique to the azimuth direction. Using the combined azimuth shift map [see Fig. 3(b)] to correct for the burst alignment, one obtains an interferogram with a continuous radar phase across both the burst and subswath boundaries (see Fig. S1 in the Supplementary Material). Features seen in the azimuth shift map in Fig. 3(b) are very similar to the “azimuth streaks” caused by ionospheric perturbations in SAR interferograms, particularly for L-band [14]. The effect of ionosphere on the interferometric phase depends on the radar wavelength and the total electron content (TEC) gradient along the satellite’s flight direction. For SAR interferometry, an apparent azimuth shift may occur if the azimuth gradients of TEC are different at the times of image acquisition. The azimuth shift caused by ionosphere perturbations is proportional to the difference of TEC gradients along the azimuth direction. Several studies have used this relationship to correct for the ionospheric effects in the L-band SAR interferometry [11], [12]. The effect of ionospheric perturbations on the C-band interferometry is expected to be much weaker than that of the L-band, as the ionospheric phase delay is inversely proportional to the square of the radar carrier wave’s frequency. Azimuth streaks, however, do occasionally occur in ERS, ENVISAT, and RADARSAT interferograms [10]. Recent studies show that the ionospheric effect on Sentinel-1 interferometry can be significant indeed [8]. Various ways have been proposed to reduce ionospheric errors in InSAR measurements, including the split range-spectrum method [8] and common-point-stacking [16]. If variations in the azimuth shift documented in this letter (see Fig. 3) are indeed due to ionospheric effects, the method proposed in this letter could be used to study the TEC variations at high spatial resolution.

It is possible that interpolation may introduce some artifacts to the phase of pixels outside of the burst overlaps. However, given that the Doppler frequency variation within a burst is small between two adjacent radar pulses, the phase error due to the interpolation of azimuth shift should be small in the nonoverlapping areas. Particularly, if the bivariate azimuth shift seen in the double-difference interferogram is indeed due to TEC gradients along the satellite flight path, the interpolation from burst overlaps to the rest of the image should be robust, as the dominant power of ionospheric phase delay usually lies at relatively large wavelengths (e.g.,  $>50$  km). At the top and bottom edges of the azimuth shift map,

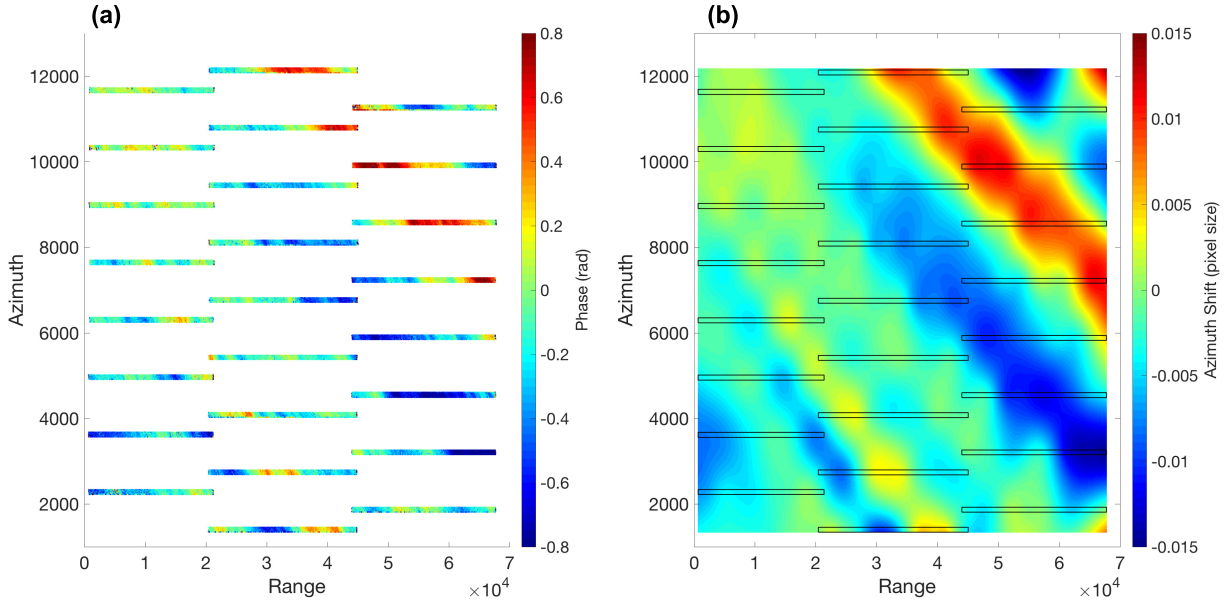


Fig. 3. (a) Double-differenced phase in the burst overlap areas of all three subswaths. (b) Interpolated azimuth shift map derived from data shown in (a). Black rectangles: bursts overlaps.

where the double-differenced phase is essentially extrapolated beyond the available burst overlaps [see Fig. 1(c)], the artifacts due to interpolation could be more pronounced. Such artifacts can be reduced by using longer radar swaths and/or trimming interferograms to exclude areas beyond the burst overlaps. Similar to conventional interferograms, an increase in temporal and geometrical baselines could deteriorate the phase correlation of a double-differenced interferogram, making the estimation of the azimuth shift less accurate. One way to mitigate this problem is to first estimate the azimuth shift maps only for interferograms with short temporal and geometric baselines and then solve for the time series of the azimuth shifts relative to a reference acquisition NESD [4].

In case of nonnegligible surface displacements along the satellite track, the proposed method is not well suited for minimizing phase discontinuities between the bursts, as contributions of surface displacements to the azimuth shift can trade off with ionospheric effects and instrument/platform-related artifacts (clock drift, orbit errors, and so on). For the same reason, the along-track interferograms obtained from interpolation of the double-differenced phase in the burst overlap areas are unlikely to be useful for measuring a low-amplitude large-wavelength along-track component of ground motion (e.g., due to interseismic deformation), despite a high theoretical accuracy of the ESD method. The along-track interferograms can provide important constraints on surface displacements that greatly exceed possible contributions from the ionosphere and/or instrument/platform artifacts (e.g., in case of large earthquakes, landslides, flow of ice, and so on), complementing measurements of range changes based on conventional interferometry.

## V. CONCLUSION

TOPS-mode SAR interferometry requires high accuracy of burst alignments. Misalignment of bursts causes phase

jumps at the burst boundaries. Geometrical burst alignment relying on precise orbits and external DEM appears sufficient for Sentinel-1A TOPS-mode interferometry in many cases. However, in many other cases, geometrical alignment is insufficient to remove phase discontinuities across burst boundaries. The ESD method was proposed to mitigate this problem. Here, we present the examples of Sentinel-1 TOPS interferograms in which neither geometrical alignment nor the ESD refinement is sufficient to remove phase discontinuities between the bursts. We propose a modification of the ESD method, named BESD that relaxes the assumption of a constant azimuth shift and estimates a point-by-point azimuth shift map that varies in both range and azimuth. We demonstrate that the BESD method is able to produce TOPS interferograms without artificial phase discontinuities. Variations in the azimuth shift in range and azimuth directions cannot be explained by clock drift or orbital errors, but may result from ionospheric perturbations during SAR acquisitions.

## ACKNOWLEDGMENT

The authors would like to thank two anonymous reviewers for their comments. Sentinel-1 data are provided by the European Space Agency through Alaska Satellite Facility and UNAVCO. SAR data processing was performed on the Comet cluster at the San Diego Supercomputing Center. Processed data and software used in this letter are available from the authors.

## REFERENCES

- [1] S. Barbot, Y. Hamiel, and Y. Fialko, "Space geodetic investigation of the coseismic and postseismic deformation due to the 2003  $M_w7.2$  Altai earthquake: Implications for the local lithospheric rheology," *J. Geophys. Res., Solid Earth*, vol. 113, p. B03403, 2008.
- [2] N. B. D. Bechor and H. A. Zebker, "Measuring two-dimensional movements using a single InSAR pair," *Geophys. Res. Lett.*, vol. 33, p. L16311, 2006.

- [3] F. D. Zan and A. Monti Guarneri, "TOPSAR: Terrain observation by progressive scans," *IEEE Trans. Geosci. Remote Sens.*, vol. 44, no. 9, pp. 2352–2360, Sep. 2006.
- [4] H. Fattah, P. Agram, and M. Simons, "A network-based enhanced spectral diversity approach for TOPS time-series analysis," *IEEE Trans. Geosci. Remote Sens.*, vol. 55, no. 2, pp. 777–786, Feb. 2017.
- [5] J. Fernández, D. Escobar, H. Peter, and P. Féménias, "Copernicus POD service operations—Orbital accuracy of Sentinel-1A and Sentinel-2A," in *Proc. Int. Symp. Space Flight Dyn.*, 2015, pp. 1–14.
- [6] Y. Fialko and J. Pearse, "Sombrero uplift above the altiplano-puna magma body: Evidence of a ballooning mid-crustal diapir," *Science*, vol. 338, no. 6104, pp. 250–252, 2012.
- [7] J. Galetzka *et al.*, "Slip pulse and resonance of the Kathmandu basin during the 2015 Gorkha earthquake, Nepal," *Science*, vol. 349, no. 6252, pp. 1091–1095, 2015.
- [8] G. Gomba, F. R. González, and F. De Zan, "Ionospheric phase screen compensation for the Sentinel-1 TOPS and ALOS-2 ScanSAR modes," *IEEE Trans. Geosci. Remote Sens.*, vol. 55, no. 1, pp. 223–235, Jan. 2017.
- [9] R. Grandin, E. Klein, M. Métois, and C. Vigny, "Three-dimensional displacement field of the 2015  $M_w$  8.3 Illapel earthquake (Chile) from across- and along-track Sentinel-1 TOPS interferometry," *Geophys. Res. Lett.*, vol. 43, no. 6, pp. 2552–2561, 2016.
- [10] A. L. Gray, K. E. Mattar, and G. Sofko, "Influence of ionospheric electron density fluctuations on satellite radar interferometry," *Geophys. Res. Lett.*, vol. 27, no. 10, pp. 1451–1454, 2000.
- [11] H.-S. Jung, D.-T. Lee, Z. Lu, and J.-S. Won, "Ionospheric correction of SAR interferograms by multiple-aperture interferometry," *IEEE Trans. Geosci. Remote Sens.*, vol. 51, no. 5, pp. 3191–3199, May 2013.
- [12] Z. Liu, H.-S. Jung, and Z. Lu, "Joint correction of ionosphere noise and orbital error in L-band SAR interferometry of interseismic deformation in southern California," *IEEE Trans. Geosci. Remote Sens.*, vol. 52, no. 6, pp. 3421–3427, Jun. 2014.
- [13] P. Prats-Iraola, R. Scheiber, L. Marotti, S. Wollstadt, and A. Reigber, "TOPS interferometry with TerraSAR-X," *IEEE Trans. Geosci. Remote Sens.*, vol. 50, no. 8, pp. 3179–3188, Aug. 2012.
- [14] D. Raucoules and M. de Michele, "Assessing ionospheric influence on L-band SAR data: Implications on coseismic displacement measurements of the 2008 Sichuan earthquake," *IEEE Geosci. Remote Sens. Lett.*, vol. 7, no. 2, pp. 286–290, Apr. 2010.
- [15] R. Scheiber, M. Jäger, P. Prats-Iraola, F. De Zan, and D. Geudtner, "Speckle tracking and interferometric processing of TerraSAR-X TOPS data for mapping nonstationary scenarios," *IEEE J. Sel. Topics Appl. Earth Observ. Remote Sens.*, vol. 8, no. 4, pp. 1709–1720, Apr. 2015.
- [16] E. Tymofeyeva and Y. Fialko, "Mitigation of atmospheric phase delays in InSAR data, with application to the eastern California shear zone," *J. Geophys. Res., Solid Earth*, vol. 120, no. 8, pp. 5952–5963, 2015.
- [17] B. Xu *et al.*, "Continent-wide 2-D co-Seismic deformation of the 2015  $M_w$  8.3 Illapel, Chile earthquake derived from Sentinel-1A data: Correction of azimuth co-registration error," *Remote Sens.*, vol. 8, no. 5, p. 376, 2016.
- [18] X. Xu, D. T. Sandwell, E. Tymofeyeva, A. González-Ortega, and X. Tong, "Tectonic and anthropogenic deformation at the Cerro Prieto geothermal step-over revealed by Sentinel-1A InSAR," *IEEE Trans. Geosci. Remote Sens.*, vol. 55, no. 9, pp. 5284–5292, Sep. 2017.